



Published in final edited form as:

Macromol Biosci. 2014 December ; 14(12): 1735–1747. doi:10.1002/mabi.201400360.

In Vitro Synergistic Action of Geldanamycin- and Docetaxel-Containing HPMA Copolymer-RGDfK Conjugates against Ovarian Cancer^a

Nate Larson,

TheraTarget, Inc., 615 Arapeen Dr., Suite 302-Y, Salt Lake City, UT 84108, USA

Department of Pharmaceutics and Pharmaceutical Chemistry, Center for Nanomedicine, Nano Institute of Utah, Salt Lake City, UT 84112, USA

Sarah Roberts,

TheraTarget, Inc., 615 Arapeen Dr., Suite 302-Y, Salt Lake City, UT 84108, USA

Abhijit Ray,

TheraTarget, Inc., 615 Arapeen Dr., Suite 302-Y, Salt Lake City, UT 84108, USA

Department of Pharmaceutics and Pharmaceutical Chemistry, Center for Nanomedicine, Nano Institute of Utah, Salt Lake City, UT 84112, USA

Brandon Buckway,

Department of Pharmaceutics and Pharmaceutical Chemistry, Center for Nanomedicine, Nano Institute of Utah, Salt Lake City, UT 84112, USA

Darwin L. Cheney, and

TheraTarget, Inc., 615 Arapeen Dr., Suite 302-Y, Salt Lake City, UT 84108, USA

Hamidreza Ghandehari

Department of Pharmaceutics and Pharmaceutical Chemistry, Center for Nanomedicine, Nano Institute of Utah, Salt Lake City, UT 84112, USA

Department of Bioengineering, University of Utah, University of Utah, 36 South Wasatch Drive, Salt Lake City, UT, 84112 USA

Nate Larson: nate.larson@gmail.com; Abhijit Ray: abhijit.ray@pharm.utah.edu; Brandon Buckway: brandon.buckway@hci.utah.edu; Darwin L. Cheney: darwin.cheney@utah.edu; Hamidreza Ghandehari: hamid.ghandehari@pharm.utah.edu

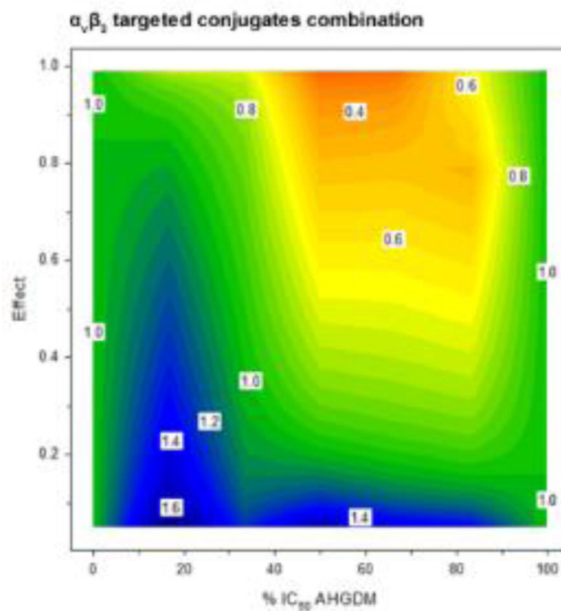
Abstract

This study describes the synthesis, characterization, and in vitro evaluation of a combination therapy utilizing HPMA copolymer-RGDfK conjugates. HPMA copolymer-RGDfK conjugates bearing either aminohexylgeldanamycin or docetaxel were synthesized and characterized. Stability was evaluated in physiologically relevant media. Binding to $\alpha_v\beta_3$ integrins on the surface of ovarian cancer cells was assessed. Cytotoxicity towards ovarian cancer cells was evaluated and the ability of the conjugates in combination to induce cell death was assessed by combination index

^aSupporting Information is available online from the Wiley Online Library or from the author.

Correspondence to: Hamidreza Ghandehari, hamid.ghandehari@pharm.utah.edu.

analysis. Conjugates bearing aminohexylgeldanamycin were more stable and exhibited slower drug release than those bearing docetaxel. Both conjugates demonstrated the ability to bind specifically to $\alpha_v\beta_3$ integrins. In combination, HPMA copolymer-RGDfK conjugates demonstrated marked synergism as compared to their non-targeted counterparts and free drug controls. HPMA copolymer-RGDfK conjugates bearing aminohexylgeldanamycin and docetaxel induce cytotoxicity in vitro in a synergistic manner, suggesting their potential as a promising combination therapy for ovarian cancer.



Keywords

geldanamycin; docetaxel; targeted drug delivery; ovarian cancer

1. Introduction

Ovarian cancer ranks fifth in cancer deaths among women, and is the most deadly cancer of the female reproductive system. In the United States, it is estimated that approximately 22,240 women will be diagnosed with, and 14,240 women will die from, ovarian cancer in 2013.^[1] Despite treatment via surgery and standard platinum/taxane chemotherapy, the estimated five year survival rate remains less than 35%.^[2, 3] More specifically, only 50% of patients diagnosed with late stage ovarian cancers who receive cisplatin/paclitaxel, the “standard of care”, will achieve clinical remission.^[4] Even so, the majority of those who experience significant clinical response will eventually relapse.^[5, 6] Thus, more effective treatments are desperately needed, especially for those diagnosed with late stage, metastatic disease.

Docetaxel (Taxotere[®]), is a semi-synthetic anti-mitotic chemotherapeutic of the taxane family that stabilizes microtubules necessary for cell division by binding β -tubulin, resulting in cell-cycle arrest and induction of apoptosis.^[7] It is currently approved for marketing in

the United States for the treatment of patients with cancers of the breast, lungs, prostate, gastro-intestinal tract, and head and neck. Compared to its taxane predecessor paclitaxel (Taxol[®]), docetaxel provides superior *in vitro* cytotoxicity^[8] and has greater potency with regard to tubulin promotion and inhibition of depolymerization.^[9] Docetaxel has proven effectiveness in combination with other traditional chemotherapeutics^[10–12] and does not demonstrate complete cross resistance with paclitaxel.^[13–15] Docetaxel is also currently under clinical investigation for the treatment of a number of cancers^[10, 16, 17] including ovarian cancer.^[18–21] However, the clinically approved formulation for intravenous administration of docetaxel (Taxotere[®]) contains polysorbate 80 as a solubilizing agent, which has been associated with acute hypersensitivity reactions, and excessive fluid retention resulting in peripheral edema.^[22, 23]

Geldanamycin and its analog stanespimycin (17-AAG, 17-(allylamino)-17-demethoxygeldanamycin) and aminohexylgeldanamycin (AHGDM, 17-(6-aminohexylamino)-17-demethoxygeldanamycin) are benzoquinoidansamycins that bind and inhibit heat shock protein 90 (HSP90).^[24] HSP90 is a molecular chaperone which maintains the stability and facilitates refolding of a number of cancer related proteins including HER-2/*neu*, Akt, Raf-1, Bcr-Abl, v-src, and mutated p53.^[25–30] HSP90 inhibitors have been widely investigated as anticancer agents due to their potential to inhibit multiple pathways involved in cancer cell survival and proliferation. Despite such potential, clinical investigation of HSP90 inhibitors such as geldanamycin and its derivatives have demonstrated significant hepatotoxicity,^[31] limiting their further development. In addition, geldanamycin and its derivatives (i.e., 17-AAG) are poorly water soluble due to their hydrophobicity,^[32] adding additional formulation challenges that need to be overcome before a clinically acceptable drug product can be obtained.

Conjugation of anti-cancer agents to water soluble polymeric carriers is one strategy that can be utilized to overcome these limitations.^[33, 34] It has been clearly demonstrated that via conjugation, the aqueous solubility of many poorly water soluble drugs, including anti-cancer agents, can be substantially increased.^[35] Also, stable conjugation to a polymeric carrier provides for opportunities to alter drug pharmacokinetics and biodistribution. The latter is of particular importance in anti-cancer therapy since treatment is often limited by toxicities observed in major organs such as the liver or kidneys. Polymeric conjugates larger than approximately 40 kDa have demonstrated the ability to evade renal filtration, allowing a higher total systemic exposure for a given dose.^[36] The resulting long blood circulation times allow such conjugates to potentially accumulate in tumor tissues via the “enhanced permeability and retention” (EPR) effect due to the disorganized tumor vasculature and underdeveloped lymphatic system of the tumor.^[37] Increased sequestration in tumors and decreased accumulation in major organs translates to a wider therapeutic index for the chemotherapeutic, potentially allowing for increases in the maximum tolerated dose (MTD) to be achieved, while maintaining a manageable toxicity profile.

Copolymers of *N*-(2-hydroxypropyl)methacrylamide (HPMA) are attractive as drug carriers due to their synthetic simplicity and wide versatility.^[38, 39] Stability during systemic circulation and site specific drug release can be obtained when chemotherapeutics are attached to the polymer backbone via enzymatically degradable peptide sequences (e.g.,

Gly-Phe-Leu-Gly (GFLG)).^[40, 41] Several anticancer HPMA copolymer-drug conjugates have been evaluated in clinical trials for the treatment of a variety of solid tumors.^[42] However, results demonstrated that while the conjugates were well tolerated, even at high drug doses, efficacy remained marginal.^[43] Therefore, additional strategies are needed to further increase tumor accumulation in an effort to achieve a more efficacious clinical response.

One approach that can successfully be utilized to increase the tumor accumulation of drug carriers is the inclusion of targeting moieties. Carriers such as liposomes,^[44] micelles,^[45] inorganic nanoparticles,^[46] and linear polymers^[33, 47, 48] can be covalently bound to antibodies, antibody fragments, peptides, and other small molecules which bind to cancer specific cell surface receptors and facilitate cellular internalization. Previously, we have demonstrated that inclusion of cyclic Arg-Gly-Asp (RGD) peptides into the side chains of HPMA copolymer-drug conjugates bearing the anticancer agents docetaxel^[49] or aminohexylgeldanamycin (AHGDM)⁵⁰ facilitated their binding to $\alpha_v\beta_3$ integrins expressed on the surface of endothelial cells of the neo-vasculature in solid tumors. This anti-angiogenic targeting strategy resulted in increases in tumor accumulation and efficacy as measured by tumor regression^[49, 50] In addition, the MTD was increased for the HPMA copolymer-drug conjugates as compared to administration of free drug, therefore allowing for additional improvements in efficacy. Elevated expression of $\alpha_v\beta_3$ integrins occurs not only on developing endothelial cells, but on the surface of cancer cells^[51–53], including ovarian cancer^[54, 55]. We therefore anticipate additional specificity for ovarian cancer tumors by utilizing this RGD targeting strategy. Anticancer strategies employing a combination of chemotherapeutics have proven very successful with substantial improvements in patient outcomes observed across an array of cancers as compared to monotherapy strategies. Such combination strategies allow inhibition of multiple cancer pathways, and when chosen carefully, can result in marked synergism of the combination treatment. The potential for an effective combination therapy utilizing an anti-angiogenic approach in ovarian cancer is supported by a reported study, the OCEANS trial,^[56] wherein bevacizumab (an anti-angiogenic monoclonal antibody against vascular endothelial growth factor A (VEGF-A) was added to carboplatin and gemcitabine for women with the first recurrence of ovarian cancer. Results indicated a greater reduction in risk of disease progression and an improvement in overall survival.

A rationally designed combination approach utilizing taxanes (e.g., docetaxel) and HSP90 inhibitors (e.g., AHGDM) has potential as a treatment option in late stage ovarian cancer. Cancer related client proteins of HSP90 such as erbB1, erbB2, epidermal growth factor receptor (EGFr), and HER-2/*neu* are over expressed in a variety of cancers including ovarian cancer following chemotherapy treatment,^[57] and have been correlated with the development of drug resistance and decreases in patient survival.^[58] It is therefore proposed that drug resistance to a potent chemotherapeutic such as docetaxel can be minimized by co-administration with a HSP90 inhibitor such as AHGDM. This hypothesis is supported by previous studies wherein a combination treatment of 17-AAG and paclitaxel resulted in a five- to 22-fold enhancement of paclitaxel cytotoxicity in non-small cell lung carcinoma (NSCLC).^[59] The combination resulted in significant reduction in tumor progression and an

extension in mean survival time from 6.5 weeks for paclitaxel alone to 19 weeks for the combination treatment.^[59] Combination strategies utilizing HSP90 inhibition and taxane chemotherapy have also demonstrated positive results in ovarian^[60] and breast^[61] cancer models.

The current study is focused on the synthesis and *in vitro* evaluation of a combination strategy utilizing $\alpha_v\beta_3$ targeted HPMA copolymer-drug conjugates bearing the anticancer agents docetaxel or aminohexylgeldanamycin (AHGDM). Following synthesis and physicochemical characterization, critical polymer-drug conjugate characteristics such as stability were evaluated, along with the ability of the conjugates to actively bind to $\alpha_v\beta_3$ integrins on the surface of ovarian cancer cells. Specifically, we evaluated a combination of: 1) free drugs, 2) non-targeted conjugates, and 3) $\alpha_v\beta_3$ targeted conjugates. Cytotoxicity of the combination treatments were evaluated against ovarian cancer cells and combination index analysis was performed to determine if the treatment is synergistic, additive, or antagonistic.

2. Experimental Section

2.1 Materials

Geldanamycin (NSC 122750) was supplied by the National Cancer Institute Developmental Therapeutics Program (NCI DTP). Docetaxel was provided by AK Scientific (Mountain View, CA). ¹²⁵I-echistatin was obtained from PerkinElmer (Waltham, MA). *N*-(2-hydroxypropyl)methacrylamide (HPMA);^[62]*N*-methacryloylglycylglycyl-p-nitrophenyl ester (MA-GG-ONp);^[63]*N*-methacryloyl-glycylphenylalanylleucylglycine (MA-GFLG-OH);^[64]*N*-methacryloyl-glycylphenylalanylleucylglycine-p-nitrophenyl ester (MA-GFLG-ONp);^[64] and *N*-methacryloyl-tyrosinamide (MA-Tyr-CONH₂)^[65] were synthesized and characterized according to previously described methods. Conjugation of the anticancer agents docetaxel (DOC) and AHGDM to produce the drug monomers MA-GFLG-DOC and MA-GFLG-AHGDM was carried out as previously described.^[49, 66]

Aminohexylgeldanamycin (AHGDM) was prepared from geldanamycin as previously described.^[66] The $\alpha_v\beta_3$ integrin binding cyclic peptide RGDfK was obtained from New England Peptide, Inc. (Boston, MA) and the peptide containing comonomer *N*-methacryloylglycylglycyl-RGDfK (MA-GG-RGDfK) was synthesized as previously described.^[49]

2.2 Synthesis and Characterization of HPMA Copolymer Conjugates

HPMA copolymers were synthesized via free radical copolymerization of comonomers in anhydrous acetone:DMSO [80:20] using *N*, *N*'-azobisisobutyronitrile (AIBN) as the initiator. A non-aqueous system was used to prevent hydrolysis of the copolymers and DMSO was incorporated to prevent precipitation and premature termination during polymerization. The targeting peptide RGDfK was incorporated via synthesis of the comonomer MA-GG-RGDfK and subsequent copolymerization (see Table 1 for feed ratios) for HPMA copolymer-DOC conjugates. For HPMA copolymer-AHGDM conjugates, RDGfK was incorporated after polymerization via side chain aminolysis of ONp groups that were introduced via copolymerization of MA-GG-ONp (Table 1). Untargeted DOC

conjugates were obtained by exclusion of MA-GG-RGDfK during polymerization. The feed composition of comonomers for all copolymers is given in Table 1 and a representative structure is shown graphically in Figure 1. Polymerization was performed in a sealed environment under N₂ gas and the temperature was maintained at 50°C for 24 h. Post polymerization, the polymers were precipitated and washed repeatedly in diethyl ether. For AHGDM conjugates, p-nitrophenol (ONp) ester content in the polymeric precursors was assessed by release of ONp from the copolymer in mild, basic aqueous conditions and quantification of released ONp by UV spectrophotometry at 400 nm. To obtain AHGDM untargeted conjugates, ONp was released from polymeric precursors in basic aqueous conditions and dialyzed against distilled water using a 3.5 kDa molecular weight cut-off (MWCO) regenerated cellulose dialysis membrane

(Spectrum Laboratories, Inc., Rancho Dominguez, CA). Control HPMA copolymers (without active agents) were also synthesized with and without RGDfK in a similar manner.

Apparent weight average molecular weight (M_w) and polydispersity (M_w/M_n) were estimated by size exclusion chromatography (SEC) on a Superose 6 column (10 mm × 30 cm) (GE Healthcare, Piscataway, NJ) using a Fast Protein Liquid Chromatography (FPLC) system (GE Healthcare). The Superose 6 column was previously calibrated with fractions of known molecular weight HPMA copolymers containing 2 mol% FITC for UV detection. All conjugates were extensively dialyzed against DI water and the absence of free AHGDM or DOC was confirmed by FPLC and HPLC (Figures S1, S2). AHGDM content was determined spectrophotometrically at 332 nm. DOC content was measured following enzymatic release of DOC by papain followed by quantification of free DOC as previously described.^[49] Briefly, 10 μL of a 25 mg/ml solution of polymer in DMSO was incubated in a mixture of 20 μl 0.1 M citrate-phosphate buffer containing 2 mM EDTA at pH 6.0 and 100 μl of the same buffer supplemented with 10 mM reduced glutathione and 0.6 mM papain. The solution was kept at 37°C for 24 h and stirred periodically. Sample was then removed, diluted 10 fold in DI water:acetonitrile [65:35], and analyzed for released DOC by HPLC. RGDfK content was quantified by amino acid analysis (University of Utah Core Research Facilities, Salt Lake City, UT).

2.3 HPLC Analysis

For DOC analysis, mobile phase consisted of deionized water and acetonitrile (ACN) using the following gradient: 0 min, 35% ACN; 15 min, 65% ACN; 25 min, 75% ACN; 30 min 95% ACN; 39 min, 100% ACN; 40 min 65% ACN. HPLC analyses were performed at 230 nm with an Agilent series 1100 HPLC (Agilent Technologies, Wilmington, DE, USA) equipped with an Alltima C18 5 μm 150 × 4.6 mm column.

HPLC analyses for AHGDM were performed with the same Agilent 1100 HPLC system equipped with a photo diode array detector set at 350 nm for quantification of AHGDM using a Waters × Bridge column (C18, 4.6 × 250mm, 5μm) and an isocratic mobile phase of 50 mM NH₄C₂H₃O₂: Acetonitrile [65: 35].

2.4 Stability and drug release of AHGDM and DOC Conjugation with HPMA Copolymers

Stability in terms of drug release from HPMA copolymer conjugates was evaluated in phosphate buffered saline (PBS) pH 7.4 and 50% mouse plasma in PBS. AHGDM and DOC equivalent concentrations were maintained at low concentrations (< 300 µg/ml and < 15 µg/ml, respectively) to prevent saturation. Samples were incubated at 37°C with periodic agitation and 100 µl aliquots sampled at each time point. AHGDM samples were extracted 3 times with 100 µl dichloromethane and dried under nitrogen. The resulting residue was re-dissolved in HPLC mobile phase and 20 µl injected for analysis. DOC samples were precipitated with 500 µl ethanol and centrifuged for 20 min at 7500 rpm. The supernatant was collected, evaporated, and resuspended in 100 µl 50 mM NaH₂PO₄ pH 7.0 buffer and extracted 3 times with 100 µl dichloromethane. The organic layer was then dried under nitrogen, re-dissolved in HPLC mobile phase and 20 µl injected for analysis. Free AHGDM and DOC dissolved in minimal DMSO was used to assess the extraction efficiency of these methods. AHGDM and DOC were successfully recovered using these methods with > 97% and > 90% efficiency, respectively. Cumulative drug release was calculated and reported as a function of time. Conjugates dissolved in mobile phase alone were analyzed by HPLC and used to determine concentrations of free drugs present at time zero. Stability experiments were performed in triplicate, with 3 samples analyzed per experiment. Release of the drugs were also evaluated using the model lysosomal enzyme cathepsin B for p-AHGDM-RGDfK and p-DOC-RGDfK as described previously.^[71]

2.5 Cell Culture

The A2780 human ovarian cancer cell line was obtained from ATCC (Manassas, VA) and cultured at 37°C in a humidified atmosphere of 5% CO₂ in RPMI-1640 cell culture medium (ATCC) supplemented with 10% fetal bovine serum (FBS) (Thermo Scientific HyClone, Logan, UT). The OVCAR-3 human ovarian cancer cell line was also obtained from ATCC and cultured in RPMI-1640 cell culture medium supplemented with 20% FBS and 0.01 mg/ml bovine insulin. Cells were maintained in a logarithmic growth phase during all studies.

2.6 Competitive Binding Affinity of HPMA Copolymers to $\alpha_v\beta_3$ Integrins

The comparative binding affinities of free RGDfK peptide and HPMA copolymer conjugates were assessed using a competitive binding assay to $\alpha_v\beta_3$ integrins expressed on the cell surface of A2780 human ovarian cancer cells. Cells were harvested, washed with PBS, and re-suspended in binding buffer (20 mmol/l tromethamine, pH 7.4, 150 mmol/l NaCl, 2 mmol/l CaCl₂, 1 mmol/l MgCl₂, 1 mmol/l MnCl₂, 0.1% bovine serum albumin). Suspended cells were added to 1.2 µm pore size 96-well Multiscreen HV filter plates (Millipore, Billerica, MA) at 100,000 cells per well. They were co-incubated at 4°C with \approx 0.05 nM ¹²⁵I-echistatin and increasing RGDfK equivalent concentrations of copolymer conjugates or free RGDfK peptide between 0 and 500 µM. After 1 h, incubation was discontinued and medium was removed by vacuum filtration using a multiscreen vacuum manifold (Millipore). Retained cells were washed 5 times with binding buffer. Filters were collected and radioactivity determined using a Cobra Auto-Gamma-counter (Canberra Industries, Inc., Meriden, CT). Binding percentage relative to cells incubated with ¹²⁵I-

echistatin alone was calculated and non-linear regression analysis and determination of IC_{50} values were carried out using GraphPad Prism (GraphPad Software, Inc., La Jolla, CA). Incubation with non-targeted copolymer conjugates was also performed at equivalent polymer concentrations to serve as negative controls. Experiments were performed in triplicate, with 3 samples analyzed per experiment.

2.7 Single Agent In Vitro Cytotoxicity

The ability of the HPMA copolymer-drug conjugates to inhibit the growth of A2780 and OVCAR-3 human ovarian cancer cell lines was evaluated *in vitro* using a 2-(2-methoxy-4-nitrophenyl)-3-(4-nitrophenyl)-5-(2,4-disulfophenyl)-2H-tetrazoliummonosodium salt (WST-8) cell viability assay (Dojindo Molecular Technologies, Inc., Rockville, MD). Due to the poor water solubility of the free drugs AHGDM and DOC, cell culture medium containing 0.5 % (v/v) DMSO was used to prevent drug precipitation. A2780 or OVCAR-3 cells (4,000 or 15,000 cells per well, respectively) were plated in 96-well plates for 24 h followed by 48 or 96 h of incubation with HPMA copolymer-drug conjugates or controls. For each treatment case, drug concentrations were varied to include data points ranging from non-toxic to highly toxic. Medium was then removed and cell viability quantified by WST-8 assay (modified MTT assay) using a SpectraMax M2 microplate UV spectrophotometer (Molecular Devices, Sunnyvale, CA). Relative viability was calculated by normalization of UV absorbance against untreated cells in each plate. Relative viability as a function of log drug concentration was plotted and nonlinear least-squares regression analysis and calculation of IC_{50} values were performed using GraphPad Prism. Experiments were performed in triplicate, with 3 samples analyzed per experiment.

2.8 In Vitro Combination Treatment and Combination Index Analysis

The combination treatments of AHGDM + DOC (free drug combination), p-AHGDM + p-DOC (non-targeted conjugate combination), and p-AHGDM-RGDfK + p-DOC-RGDfK (targeted conjugate combination) were evaluated against A2780 cells *in vitro*. Relative viability as compared to untreated cells as determined by CCK-8 assay served as the primary endpoint. For each combination treatment, various drug ratios of AHGDM/DOC corresponding to 83% IC_{50} AHGDM + 17% IC_{50} DOC, 67% IC_{50} AHGDM + 33% IC_{50} DOC, 50% IC_{50} AHGDM + 50% IC_{50} DOC, 33% IC_{50} AHGDM + 67% IC_{50} DOC, and 17% IC_{50} AHGDM + 83% IC_{50} DOC were evaluated. Cells were treated in a “pulse chase” manner via 4 h incubation with combination doses ranging from non-toxic to highly toxic. Following treatment, cells were washed with PBS and incubation continued until terminal assessment of cell viability. Drug effect was defined as $(1 - [\% \text{ relative viability } 100^{-1}])$. Combination index analysis was performed with CalcuSyn combination index software (Biosoft, Inc.) based on the Chou-Talalay method.^[67] Contour plots with drug ratio on the x-axis, effect on the y-axis, and combination index on the z-axis were plotted for each combination treatment using SigmaPlot 11.0 (Systat Software, Inc.). Experiments were performed in triplicate, with 3 samples analyzed per experiment.

2.9 Statistical Analysis

Differences in binding affinity and *in vitro* growth inhibition IC₅₀ values were determined by one-way ANOVA. Where differences were detected, Tukey's post-test was used to test for significance between groups. The default significance level was set at $\alpha=0.05$ for all statistical tests.

3. Results and Discussion

3.1. Synthesis and Characterization of HPMA Copolymer Conjugates

All HPMA copolymer-drug conjugates were synthesized by free radical copolymerization using AIBN as the initiator and physicochemical characteristics are given in Table 1. Estimated molecular weights for all of the conjugates synthesized was maintained below 45 kDa to allow renal elimination in an *in vivo* setting^[68] and the feed compositions of drug containing monomers for AHGDM and DOC conjugates were kept at 5.0 and 2.5 mol%, respectively, to ensure aqueous solubility based on previous observations. The amount of RGDfK peptide was also maintained at approximately 20 wt%, a level where previous conjugates demonstrated sufficient active binding to $\alpha_v\beta_3$ integrins and *in vivo* targeting ability.^[49, 50, 69, 70] The resulting conjugates had a wider molecular weight distribution, with polydispersities ranging from 1.6 to 1.9.

For AHGDM conjugates, conjugation of RGDfK to the polymer backbone via the Gly-Gly linker occurred post-polymerization via aminolysis of p-nitrophenol groups and non-targeted conjugates were obtained following hydrolysis of the same. The method resulted in copolymers with significant negative charge due to the presence of free carboxyl groups, which potentially altered biodistribution and pharmacokinetics. However, this charge also imparted significant water solubility to the conjugates. There was therefore a balance between charge and solubility that was considered in the design of these conjugates, and further studies will be required to optimize these parameters. Conjugation of RGDfK to polymers containing DOC in the side chains, on the other hand, occurred via synthesis of the comonomer MA-GG-RGDfK followed by copolymerization. This route for RGDfK inclusion was preferred due to the potential for docetaxel to be released from the polymer backbone during aminolysis. However, this method resulted in a slightly lower RGDfK conversion rate of 67%, as compared to 82% obtained for AHGDM conjugates via aminolysis, where conversion rate is defined as the percent incorporation achieved as compared to the theoretical amount achievable based on the feed ratios used. This was most likely due to solubility limitations of the MA-GG-RGDfK comonomer encountered during copolymerization, but could also be due to differences in the reactivity ratios of the comonomers. Control HPMA copolymers were also synthesized with similar physicochemical characteristics to investigate the effect of drug conjugation on RGDfK binding affinity and for use as controls in *in vitro* cytotoxicity studies.

3.2. Stability and drug release of AHGDM and DOC Conjugation with HPMA Copolymers

The stability of polymer-drug conjugates is of utmost concern, as it is critically important for the conjugate to remain stable during systemic circulation. If drug release occurs prematurely, safety can be compromised. Previously, we have reported that HPMA

copolymer-drug conjugates utilizing the GFLG degradable spacer are cleaved in the presence of the lysosomal enzyme cathepsin B.^[66] Drug release occurs for both amide linked drugs like AHGDM and ester linked drugs like DOC. This mechanism of release occurs within lysosomes and is responsible for drug release following cellular uptake. If degradation of the active agent occurs prematurely, efficacy can be compromised. The stability of AHGDM and DOC conjugates was therefore evaluated in two biologically relevant media wherein drug release as a function of time was quantified by HPLC.

The release in phosphate buffered saline (PBS) pH 7.4 was first evaluated (Figure 2a). Very minimal release was observed for AHGDM conjugates, with less than 2% released over a period of 24 h. Drug conjugation, in this case, was performed between the amino end of AHGDM and the carboxyl terminus of the GFLG degradable spacer, resulting in a stable amide linkage (See Figure 1). More moderate drug release was observed for DOC conjugates, with approximately 35% released over 24 h, with a consistent average release rate ($r^2 > 0.99$ by linear regression) of approximately 1.4% per hr. In this case, drug conjugation was performed between a hydroxyl group of DOC and the carboxy terminus of the GFLG spacer, resulting in a less stable ester linkage that was more prone to hydrolysis³⁸, especially in basic, aqueous conditions. This elevated drug release was therefore most likely the result of the slightly basic pH of the PBS, which facilitated hydrolysis over time.

Next, to better represent the stability of the conjugates during *in vivo* circulation, drug release was assessed in 50% mouse plasma in PBS (Figure 2b). Although a similar trend was observed with DOC conjugates demonstrating faster drug release than AHGDM conjugates, the overall rates of release were increased for all. For AHGDM conjugates, the average rate of release was approximately 0.6% per h and the average rate of release for DOC conjugates was approximately 11% per h. While it is acknowledged that the DOC conjugates show some instability, previous work^[49, 50, 69] demonstrated that when using a combination of HPMA copolymers below renal threshold and $\alpha_v\beta_3$ integrin targeting, accumulation of the conjugates in solid tumors occurs within a short time frame (1–2 h), while the majority of the remainder of the dose was eliminated via renal excretion. Thus, we anticipate that this level of instability will not have a major effect on either safety or efficacy. Additionally, previous results demonstrated tolerability and efficacy of $\alpha_v\beta_3$ integrin targeted HPMA copolymer-DOC conjugates in a human prostate cancer xenograft mouse model.⁴⁹

In all stability studies, no significant differences in drug release were observed between non-targeted conjugates and $\alpha_v\beta_3$ targeted conjugates bearing the RGDfK peptide. Both the RGDfK peptide and the remainder of the polymeric conjugate were relatively hydrophilic, thus no significant changes in the polymer conformation was expected. Thus, it was anticipated that access to the enzymatic cleavage site would remain similar, resulting in similar release rates. Drug release studies were also performed in order to confirm that the Cathepsin B based enzymatic cleavage of GFLG is intact for both targeted HPMA copolymer conjugates. The *in vitro* release assay demonstrated an early burst release within the first 15 min and $20.98 \pm 0.4\%$ and $30.98 \pm 2.3\%$ release of the p-AHGDM-RGDfK and p-DOC-RGDfK within 3 hrs, respectively (Figure S5). These release rates are similar to release rates previously reported.^[71]

3.3 Competitive Binding Affinity of HPMA Copolymers to $\alpha_v\beta_3$ Integrins

As previously discussed, the conjugation of targeting peptides to the side chains of HPMA copolymers provided for potential increases in the therapeutic index for a given chemotherapeutic, and therefore offered an opportunity to maximize efficacy while minimizing toxicity. Inclusion of the RGD sequence directed binding to $\alpha_v\beta_3$ integrins expressed on the surface of angiogenic blood vessels in developing solid tumors. In previous work, we demonstrated that inclusion of the cyclic RGDfK peptide in the side chains of HPMA copolymer-drug conjugates facilitated binding to $\alpha_v\beta_3$ integrins expressed on the surface of human vascular endothelial cells (HUVECs).^[49, 71] It was also reported that expression of $\alpha_v\beta_3$ integrins occurred in a variety of cancer cells including ovarian cancer cells.^[72] Therefore, our aim was to demonstrate that these targeted conjugates also had the ability to bind ovarian cancer cells in addition to their already established ability to target endothelial cells. A competitive binding assay was performed in which A2780 cells were co-incubated with increasing concentrations of the conjugates and a fixed concentration of ¹²⁵I-radiolabel echistatin, a known binder for $\alpha_v\beta_3$ integrins. When compared to the binding of free RGDfK peptide, a measure of the relative binding affinity was calculated, which corresponded to the degree in which the binding affinity of RGDfK was decreased following conjugation.

All conjugates bearing RGDfK peptides demonstrated competitive binding to $\alpha_v\beta_3$ integrins (Figure 3). However, for AHGDM and DOC conjugates, relative binding affinity was reduced from 2 μ M for free RGDfK peptide to 62 μ M and 46 μ M, respectively, whereas the control copolymer bearing RGDfK (p-RGDfK) showed only a marginal reduction to 10 μ M (Figure 3). This can possibly be explained due to potential differences in the hydrophobicity of the conjugates, which in turn can impact their physical conformation while in solution. Hydrophobic intramolecular interactions between drug molecules may cause the conjugates to adopt a more compact conformation. This effect, coupled with the fact that these were produced via random copolymerization, may result in the exclusion of RGD motifs from the conjugate surface, thereby reducing binding affinity on an RGDfK molar basis. When drug molecules are absent (as in the control copolymer p-RGDfK), the conjugate can retain a more extended, random-coil form where the RGD motifs are more accessible for interactions with $\alpha_v\beta_3$ integrins, resulting in a lesser reduction in the binding affinity. Incubation with non-targeted HPMA copolymer-drug conjugates was included in these studies as negative controls. At equivalent polymer mass concentrations, all non-targeted conjugates (without RGDfK peptides) demonstrated no evidence of competitive binding (Figure 3). Therefore, competition with echistatin observed for $\alpha_v\beta_3$ targeted conjugates was due to the presence of RGDfK peptides.

3.4 Single Agent In Vitro Cytotoxicity

The ability of the conjugates to inhibit the growth of A2780 and OVCAR-3 human ovarian cancer cells *in vitro* was evaluated using a WST-8 cell viability assay. The A2780 cell line was established from tumor tissue of an untreated patient, whereas the OVCAR-3 cell line, established from a previously treated patient, was resistant to clinically relevant concentrations of adriamycin, melphalan, and cisplatin, and considered an appropriate model in which to study drug resistance in ovarian cancer. Our results did not indicate overall

trends in differences in the susceptibility of these cell lines to HPMA copolymer-drug conjugates, or the free drugs AHGDM and DOC (Figure 4).

Results are summarized in Figure 4, and detailed results are provided in the Supporting Information (Figures S3,S4). DOC conjugates exhibited high potency with IC₅₀ values ranging from 1–4 nM (Figure 4). Although statistical differences were detected between A2780 and OVCAR-3 cells treated with DOC and DOC conjugates, the differences were not substantial with all IC₅₀ values remaining in the single digit nM range. AHGDM conjugates exhibited moderate potency with IC₅₀ values ranging from 3–7 μM. In this case, some interesting differences were detected. For the case of the non-targeted conjugate p-AHGDM, the potency was reduced in OVCAR-3 cells as compared to A2780 cells with IC₅₀ values of 7.2 μM and 2.9 μM, respectively ($p < 0.01$). However, this potency was essentially regained by inclusion of the RGDfK targeting peptide, with p-AHGDM-RGDfK exhibiting an IC₅₀ of 3.4 in OVCAR-3 cells as compared to p-AHGDM exhibiting an IC₅₀ of 7.2 in OVCAR-3 cells ($p < 0.05$) (Figure 4). This difference may suggest a potential advantage in overcoming drug resistance.

An interesting result was also observed, wherein free RGDfK peptide and control HPMA copolymer-RGDfK demonstrated some potency with IC₅₀ values of 4–7 μM and 16–24 μM in A2780 and OVCAR-3 cells, respectively. *In vitro* work with these systems in endothelial cells and various prostate cancer cell lines did not demonstrate any potency at similar concentrations.^[49, 71] It therefore appears that this effect is cell line dependent. It was reported that α_vβ₃ integrins can regulate cell proliferation in ovarian cancer cells through activation of integrin-linked kinase (ILK),^[73] which provides some explanation of these results. However, at this stage the exact mechanism of action is unknown, and future work is needed to elucidate how these RGD motifs are eliciting cytotoxicity.

3.5. In Vitro Combination Treatment and Combination Index Analysis

The use of multiple chemotherapeutic agents proved successful, with many first line treatment strategies for an array of cancers relying on combination strategies. When two drugs are used in combination, their overall effect can be antagonistic, additive, or synergistic. Various methods exist for determining whether a combination treatment is antagonistic, additive, or synergistic.^[74] The most commonly employed, however, is that described by Chou and Talalay.^[67] For a combination treatment of two drugs, this method requires evaluation of the effects of each drug when used individually, as well as in combination. The result is calculation of a combination index (CI) parameter. When CI is between 1 and ∞ ($CI > 1$), the combination treatment is antagonistic. When $CI = 1$, the combination treatment is additive, and when CI is between 0 and 1 ($CI < 1$), the treatment is synergistic. (Note that the absolute scales of antagonism and synergism are not equivalent.)

In the current study, combination index was evaluated as a function of drug ratio and effect. Concentrations are reported as a percentage of IC₅₀ to adjust for differences in potency between compounds. The combination treatments of AHGDM + DOC (free drug combination), p-AHGDM + p-DOC (non-targeted conjugates combination), and p-AHGDM-RGDfK + p-DOC-RGDfK (targeted conjugates combination) were evaluated via a cell viability assay. Combination treatment occurred for only 4 h in a “pulse chase” style,

wherein parameters such as drug release kinetics and cellular uptake exhibit a more profound effect on viability. For each combination treatment, various drug ratios of AHGDM/DOC corresponding to 83% IC₅₀ AHGDM + 17% IC₅₀ DOC, 67% IC₅₀ AHGDM + 33% IC₅₀ DOC, 50% IC₅₀ AHGDM + 50% IC₅₀ DOC, 33% IC₅₀ AHGDM + 67% IC₅₀ DOC, and 17% IC₅₀ AHGDM + 83% IC₅₀ DOC were evaluated. For each drug ratio, concentrations ranging from non-toxic to highly toxic were evaluated. Using this method, we were able to determine how the combination index is affected by both drug ratio and effect.

For the free drug combination (AHGDM + DOC), the combination index was approximately equal to 1 over a majority of drug ratios and effects (Figure 5). Moderate antagonism (CI = 1.2 – 1.4) was observed for the 50% IC₅₀ AHGDM + 50% IC₅₀ DOC drug ratio at effects less than 0.5, and slight synergism (CI = 0.8) was observed for the 83% IC₅₀ AHGDM + 17% IC₅₀ DOC drug ratio at effects greater than 0.5. Overall, however, the free drug combination resulted in additive effects.

For the combination treatment of non-targeted conjugates (p-AHGDM + p-DOC), moderate antagonism (CI = 1.2 – 1.4) was observed over a dose ratio ranging from 17% IC₅₀ AHGDM + 83% IC₅₀ DOC to 50% IC₅₀ AHGDM + 50% IC₅₀ DOC (Figure 5). This antagonism was also observed over a wide range of effect levels. However, the area of synergism was also increased as compared to the free drug combination, with slight synergism observed at a dose ratio of 83% IC₅₀ AHGDM + 17% IC₅₀ DOC at effects greater than 0.2.

The combination treatment with targeted conjugates (p-AHGDM-RGDfK + p-DOC-RGDfK) exhibited more distinct positive results (Figure 5). Although the region of moderate antagonism (CI = 1.2 – 1.4) was still observed at the 17% IC₅₀ AHGDM + 83% IC₅₀ DOC drug ratio at effects below 0.5, a broad region of synergism was observed for drug ratios ranging from 50% IC₅₀ AHGDM + 50% IC₅₀ DOC to 83% IC₅₀ AHGDM + 17% IC₅₀ DOC at effect levels greater than 0.5. In particular, the drug ratio of 67% IC₅₀ AHGDM + 33% IC₅₀ DOC showed the highest level of synergism (CI = 0.4) at effect levels above 0.9. This can possibly be explained by the additional effects due to presence of the RGDfK peptide, which was shown to elicit some inherent activity (Figure 4). Potential differences in the uptake rate of the $\alpha_v\beta_3$ targeted polymers due to their increased binding affinity for $\alpha_v\beta_3$ integrins and possible differences in sub-cellular pharmacokinetics and distribution due to variations in physicochemical properties of the RGDfK containing conjugates could also play a potential role. It is also possible that differences in drug release from the conjugate may play a role, as AHGDM conjugates were shown to be significantly more stable than DOC conjugates (Figure 2). Further investigation is necessary to determine the exact mechanism(s). It is also possible that saturation of $\alpha_v\beta_3$ integrins could occur, as the AHGDM and DOC conjugates are competing for the same target. Saturation is more likely to occur *in vitro*, where high localized concentrations are present, and further investigation is necessary to determine the combined effects of these systems *in vivo*. The moderate stability of the DOC conjugates may present some potential problems when applied in an appropriate *in vivo* experiment for synergism. However, previous studies have demonstrated that similar moderately stable p-DOC-HPMA conjugates demonstrated a significant anti-tumor effect

when compared to free drug in a prostate tumor disease model.^[49] Clearly, the pharmacokinetic profiles of both p-AHGDM-RGDfK and p-DOC-RGDfK would have to be determined in order to discover when the proper time of administration and dosage would be in order to mimic the synergistic tumor cell concentrations demonstrated in this *in vitro* study. The results observed here, however, are encouraging, especially given the fact that synergism seems to be maximized at higher effect levels. Thus, use of such a combination treatment can potentially induce toxicity in the vast majority of cells within a given tumor mass, resulting in more efficacious therapy. These findings are also significant given the fact that a large number of chemotherapy regimens consist of combination therapies. These results demonstrate that new, effective combination therapies can potentially be obtained through conjugation to targeted, water-soluble polymers such as HPMA, for drugs which do not demonstrate synergism when administered as small molecular weight entities.

4. Conclusions

HPMA copolymer-RGDfK conjugates bearing either AHGDM or DOC were successfully synthesized and characterized. These conjugates, which bear the RGDfK peptide, demonstrated binding to $\alpha_v\beta_3$ integrins expressed on the surface of human ovarian cancer cells and were effective in inhibiting their growth. Moderate stability was observed for DOC conjugates, wherein conjugation was via ester linkage, and high stability was observed for AHGDM conjugates, wherein conjugation was via amide linkage. Combination index analysis revealed regions of moderate antagonism and slight synergism for combination treatments of free drugs (AHGDM + DOC) and non-targeted conjugates (p-AHGDM + p-DOC). A broad region of synergism was observed for combination treatment of targeted conjugates. The optimum drug ratio was determined to be 67% IC₅₀ AHGDM + 33% IC₅₀ DOC, with combination index values ranging from 0.4 – 0.6 observed at effect levels above 0.5. These results suggest the potential utility of these carriers in combination drug delivery for the treatment of ovarian cancer.

Supplementary Material

Refer to Web version on PubMed Central for supplementary material.

Acknowledgements

This research was supported by the National Institutes of Health grants R41CA144818 and R01EB007171.

Nomenclature

17-AAG	17-(allylamino)-17-demethoxygeldanamycin
ACN	acetonitrile
AHGDM	17-(hexane-1, 6-diamine)-17-demethoxygeldanamycin
DMSO	dimethyl sulfoxide
DOC	docetaxel

EDTA	ethylenediaminetetraacetic acid
EPR	enhanced permeability and retention
FPLC	fast protein liquid chromatography
GFLG	gly-phe-leu-gly
HPLC	high performance liquid chromatography
HPMA	<i>N</i> -(2-hydroxypropyl)methacrylamide
HSP90	heat shock protein 90 kDa
MTD	maximum tolerated dose
ONp	p-nitrophenol
PBS	phosphate buffered saline
RGD	arg-gly-asp
RGDfK	cyclic arg-gly-asp- <i>D</i> -phe-lys

References

1. American Cancer Society. <http://www.cancer.org/cancer/ovariancancer/detailedguide/ovarian-cancer-key-statistics>.
2. Gonzalez-Diego P, Lopez-Abente G, Pollan M. Eur. J. Cancer. 2000; 36:1816. [PubMed: 10974630]
3. Rowland JH, Aziz N, Tesaro G, Feuer EJ. Semin. Oncol. Nurs. 2001; 17:236. [PubMed: 11764706]
4. Guarneri V, Piacentini F, Barbieri E, Conte PF. Gynecol. Oncol. 2009; 117:152. [PubMed: 20056266]
5. Gadducci A, Sartori E, Maggino T, Zola P, Landoni F, Fanucchi A, Palai N, Alessi C, Ferrero AM, Cosio S, Cristofani R. Gynecol. Oncol. 1998; 68:150. [PubMed: 9514797]
6. Gadducci A, Cosio S, Conte PF, Genazzani AR. Crit. Rev. Oncol. Hematol. 2005; 55:153. [PubMed: 15890524]
7. Fu Y, Li S, Zu Y, Yang G, Yang Z, Luo M, Jiang S, Wink M, Efferth T. Curr. Med. Chem. 2009; 16:3966. [PubMed: 19747129]
8. Montero A, Fossella F, Hortobagyi G, Valero V. Lancet Oncol. 2005; 6:229. [PubMed: 15811618]
9. Ringel I, Horwitz SB. J. Natl. Cancer Inst. 1991; 83:288. [PubMed: 1671606]
10. Belfiglio M, Fanizza C, Tinari N, Ficorella C, Iacobelli S, Natoli C. J. Cancer Res. Clin. Oncol. 2012; 138:221. [PubMed: 22095437]
11. Amarantidis K, Xenidis N, Chelis L, Chamalidou E, Dimopoulos P, Michailidis P, Tentes A, Deftereos S, Karanikas M, Karayiannakis A, Kakolyris S. Oncology. 2011; 80:359. [PubMed: 21811088]
12. Pallis AG, Agelaki S, Agelidou A, Varthalitis I, Syrigos K, Kentepozidis N, Pavlakou G, Kotsakis A, Kontopodis E, Georgoulas V. BMC Cancer. 2010; 10:633. [PubMed: 21092076]
13. Markman M, Zanotti K, Webster K, Peterson G, Kulp B, Belinson J. Gynecol. Oncol. 2003; 91:573. [PubMed: 14675679]
14. Benjapibal M, Kudelka AP, Vasuratna A, Edwards CL, Verschraegen CF, Valero V, Vadhan-Raj S, Kavanagh JJ. Anticancer Drugs. 1998; 9:577. [PubMed: 9877247]
15. Sato S, Kigawa J, Kanamori Y, Itamochi H, Oishi T, Shimada M, Iba T, Naniwa J, Uegaki K, Terakawa N. Cancer Chemother. Pharmacol. 2004; 53:247. [PubMed: 14610615]

16. Kafri Z, Heilbrun LK, Sukari A, Yoo G, Jacobs J, Lin HS, Mulrenan H, Smith D, Kucuk O. *ISRN Oncol.* 2012; 2012:159568. [PubMed: 22655205]
17. Tamura S, Imano M, Takiuchi H, Kobayashi K, Imamoto H, Miki H, Goto Y, Aoki T, Peng YF, Tsujinaka T, Furukawa H. *Anticancer Res.* 2012; 32:1403. [PubMed: 22493377]
18. Fu S, Hennessy BT, Ng CS, Ju Z, Coombes KR, Wolf JK, Sood AK, Levenback CF, Coleman RL, Kavanagh JJ, Gershenson DM, Markman M, Dice K, Howard A, Li J, Li Y, Stenke-Hale K, Dyer M, Atkinson E, Jackson E, Kundra V, Kurzrock R, Bast RC Jr, Mills GB. *Gynecol. Oncol.* 2012; 126:47. [PubMed: 22487539]
19. Garcia AA, Yessaian A, Pham H, Facio G, Muderspach L, Roman L. *Cancer Invest.* 2012; 30:295. [PubMed: 22468744]
20. Sorbe G, Graflund M, Horvath G, Swahn M, Boman K, Bangshoj R, Lood M, Malmstrom H. *Int. J. Gynecol. Cancer.* 2012; 22:47. [PubMed: 22193643]
21. Ushijima K, Kamura T, Tamura K, Kuzuya K, Sugiyama T, Noda K, Ochiai K. *Int. J. Clin. Oncol.* 2013; 18:126. [PubMed: 22127346]
22. Tan Q, Liu X, Fu X, Li Q, Dou J, Zhai G. *Expert Opin. Drug Deliv.* 2012; 9:975. [PubMed: 22703284]
23. Engels FK, Mathot RA, Verweij J. *Anticancer Drugs.* 2007; 18:95. [PubMed: 17159596]
24. Neckers L, Workman P. *Clin. Cancer Res.* 2012; 18:64. [PubMed: 22215907]
25. Kamal A, Thao L, Sensintaffar J, Zhang L, Boehm MF, Fritz LC, Burrows FJ. *Nature.* 2003; 425:407. [PubMed: 14508491]
26. Sankhala KK, Mita MM, Mita AC, Takimoto CH. *Curr. Drug Targets.* 2011; 12:2001. [PubMed: 21777196]
27. Schulte TW, Neckers LM. *Cancer Chemother. Pharmacol.* 1998; 42:273. [PubMed: 9744771]
28. Xu W, Mimnaugh E, Rosser MF, Nicchitta C, Marcu M, Yarden Y, Neckers L. *J. Biol. Chem.* 2001; 276:3702. [PubMed: 11071886]
29. Sato S, Fujita N, Tsuruo T. *Proc. Natl. Acad. Sci. U S A.* 2000; 97:10832. [PubMed: 10995457]
30. Blagosklonny MV, Toretsky J, Neckers L. *Oncogene.* 1995; 11:933. [PubMed: 7675452]
31. Sharp S, Workman P. *Adv. Cancer Res.* 2006; 95:323. [PubMed: 16860662]
32. Gorska M, Popowska U, Sielicka-Dudzina A, Kuban-Jankowska A, Sawczuk W, Knap N, Cicero G, Wozniak F. *Front. Biosci.* 2012; 17:2269.
33. Larson N, Ghandehari H. *Chem. Mater.* 2012; 24:840. [PubMed: 22707853]
34. Canal F, Sanchis J, Vicent MJ. *Curr. Opin. Biotechnol.* 2011; 22:894. [PubMed: 21724381]
35. Duncan R. *Nat. Rev. Cancer.* 2006; 6:688. [PubMed: 16900224]
36. Fang J, Nakamura H, Maeda H. *Adv. Drug Deliv. Rev.* 2011; 63:136. [PubMed: 20441782]
37. Maeda H. *J. Control Release.* 2012; 164:138. [PubMed: 22595146]
38. Duncan R, Vicent MJ. *Adv. Drug Deliv. Rev.* 2010; 62:272. [PubMed: 20005271]
39. Kopecek J, Kopeckova P. *Adv. Drug Deliv. Rev.* 2010; 62:122. [PubMed: 19919846]
40. Subr V, Kopecek J, Pohl J, Baudys M, Kostka V. *J. Control Release.* 1988; 8:133.
41. Putnam, D.; Kopecek, J. *Biopolymers II. Vol. 122.* Berlin: Springer; 1995. p. 55-123.
42. Duncan R. *Adv. Drug Deliv. Rev.* 2009; 61:1131. [PubMed: 19699249]
43. Seymour LW, Ferry DR, Kerr DJ, Rea D, Whitlock M, Poyner R, Boivin C, Hesslewood S, Twelves C, Blackie R, Schatzlein A, Jodrell D, Bissett D, Calvert H, Lind M, Robbins A, Burtles S, Duncan R, Cassidy J. *Int. J. Oncol.* 2009; 34:1629. [PubMed: 19424581]
44. Sawant RR, Torchilin VP. *AAPS J.* 2012; 14:303. [PubMed: 22415612]
45. Sutton D, Nasongkla N, Blanco E, Gao J. *Pharm. Res.* 2007; 24:1029. [PubMed: 17385025]
46. Dykman L, Khlebtsov N. *Chem. Soc. Rev.* 2012; 41:2256. [PubMed: 22130549]
47. Pike DB, Ghandehari H. *Adv. Drug Deliv. Rev.* 2010; 62:167. [PubMed: 19951733]
48. Hopewell JW, Duncan R, Wilding D, Chakrabarti K. *Hum. Exp. Toxicol.* 2001; 20:461. [PubMed: 11776408]
49. Ray A, Larson N, Pike DB, Gruner M, Naik S, Bauer H, Malugin A, Greish K, Ghandehari H. *Mol. Pharm.* 2011; 8:1090. [PubMed: 21599008]

50. Greish K, Ray A, Bauer H, Larson N, Malugin A, Pike D, Haider M, Ghandehari H. *J. Control Release.* 2011; 151:263. [PubMed: 21223983]
51. Felding-Habermann B, Mueller BM, Romerdahl CA, Cheresh DA. *J. Clin. Invest.* 1992; 89:2018. [PubMed: 1376331]
52. Bello L, Francolini M, Marthyn P, Zhang J, Carroll RS, Nikas DC, Strasser JF, Villani R, Cheresh DA, Black PM. *Neurosurgery.* 2001; 49:380. discussion 390. [PubMed: 11504114]
53. Gasparini G, Brooks PC, Biganzoli E, Vermeulen PB, Bonoldi E, Dirix LY, Ranieri G, Miceli R, Cheresh DA. *Clin. Cancer Res.* 1998; 4:2625. [PubMed: 9829725]
54. Janssen M, Oyen WJ, Massuger LF, Frielink C, Dijkgraaf I, Edwards DS, Radjopadhye M, Corstens FH, Boerman OC. *Cancer Biother. Radiopharm.* 2002; 17:641. [PubMed: 12537667]
55. Landen CN, Kim TJ, Lin YG, Merritt WM, Kamat AA, Han LY, Spannuth WA, Nick AM, Jennings NB, Kinch MS, Tice D, Sood AK. *Neoplasia.* 2008; 10:1259. [PubMed: 18953435]
56. Aghajanian C, Blank SV, Goff BA, Judson PL, Teneriello MG, Husain A, Sovak MA, Yi J, Nycum LR. *J. Clin. Oncol.* 2012; 30:2039. [PubMed: 22529265]
57. Lu X, Xiao L, Wang L, Ruden DM. *Biochem. Pharmacol.* 2012; 83:995. [PubMed: 22120678]
58. Scaltriti M, Dawood S, Cortes J. *Clin. Cancer Res.* 2012; 18:4508. [PubMed: 22718860]
59. Nguyen DM, Lorang D, Chen GA, Stewart JH IV, Tabibi E, Schrupp DS. *Ann. Thorac. Surg.* 2001; 72:371. [PubMed: 11515869]
60. Smith V, Hobbs S, Court W, Eccles S, Workman P, Kelland LR. *Anticancer Res.* 2002; 22:1993. [PubMed: 12174876]
61. Solit DB, Basso AD, Olshen AB, Scher HI, Rosen N. *Cancer Res.* 2003; 63:2139. [PubMed: 12727831]
62. Strohalm J, Kopecek J. *Makromol. Chem.* 1978; 70:109.
63. Rejmanova P, Labsky J, Kopecek J. *Makromol. Chem.* 1977; 178:2159.
64. Ulbrich K, Subr V, Strohalm J, Plocova D, Jelinkova M, Rihova B. *J. Control Release.* 2000; 64:63. [PubMed: 10640646]
65. Lee JH, Kopeckova P, Kopecek J, Andrade JD. *Biomaterials.* 1990; 11:455. [PubMed: 2242394]
66. Kasuya Y, Lu ZR, Kopeckova P, Tabibi SE, Kopecek J. *Pharm Res.* 2002; 19:115. [PubMed: 11883637]
67. Chou TC, Talalay P. *Adv. Enzyme Regul.* 1984; 22:27. [PubMed: 6382953]
68. Lammers T, Kuhnlein R, Kissel M, Subr V, Etrych T, Pola R, Pechar M, Ulbrich K, Storm G, Huber P, Peschke P. *J. Control Release.* 2005; 110:103. [PubMed: 16274831]
69. Borgman MP, Aras O, Geysler-Stoops S, Sausville EA, Ghandehari H. *Mol. Pharm.* 2009; 6:1836. [PubMed: 19743884]
70. Mitra A, Mulholland J, Nan A, McNeill E, Ghandehari H, Line BR. *J. Control Release.* 2005; 102:191. [PubMed: 15653145]
71. Borgman MP, Ray A, Kolhatkar RB, Sausville EA, Burger AM, Ghandehari H. *Pharm. Res.* 2009; 26:1407. [PubMed: 19225872]
72. Gamble LJ, Borovjagin AV, Matthews QL. *Exp. Ther. Med.* 2010; 1:233. [PubMed: 21494315]
73. Cruet-Hennequart S, Maubant S, Luis J, Gauduchon P, Staedel C, Dedhar S. *Oncogene.* 2003; 22:1688. [PubMed: 12642872]
74. Chou TC. *Cancer Res.* 2010; 70:440. [PubMed: 20068163]

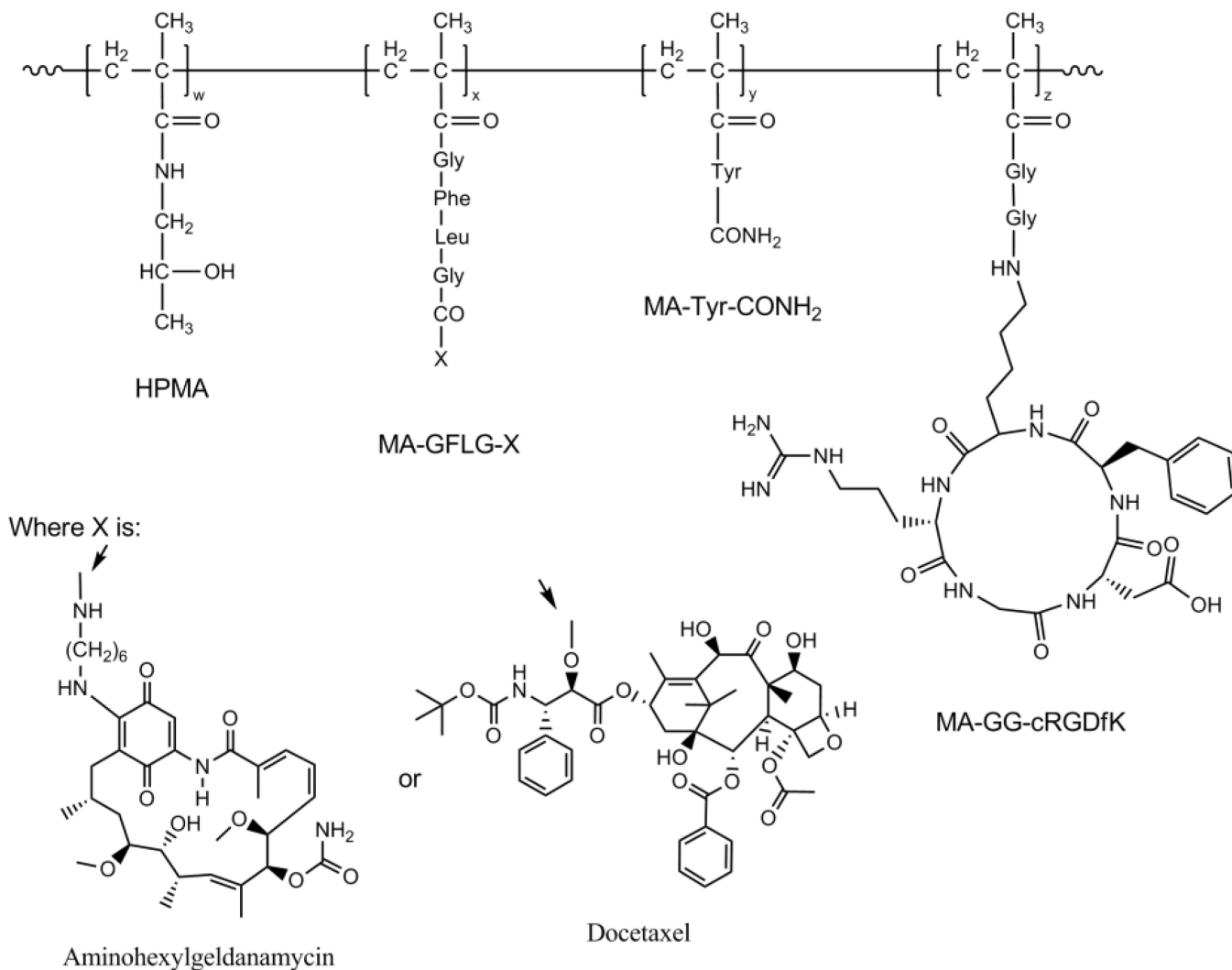


Figure 1. Representative structure of $\alpha_v\beta_3$ targeted HPMA copolymer-drug conjugates
 Random copolymers are comprised of four functional monomers: 1) HPMA, which makes up the primary backbone and increases hydrophilicity and aqueous solubility, 2) MA-GFLG-X, where X is either aminohexylgeldanamycin or docetaxel bound to the lysosomally degradable drug linker GFLG via an amide or ester linkage respectively, 3) MA-Tyr-CONH₂, a modified tyrosine to facilitate radiolabeling in future studies, and 4) MA-GG-cRGDfK, which contains the cyclic peptide RGDFK which binds to $\alpha_v\beta_3$ integrins expressed on the surface of ovarian tumor cells and neovasculature.

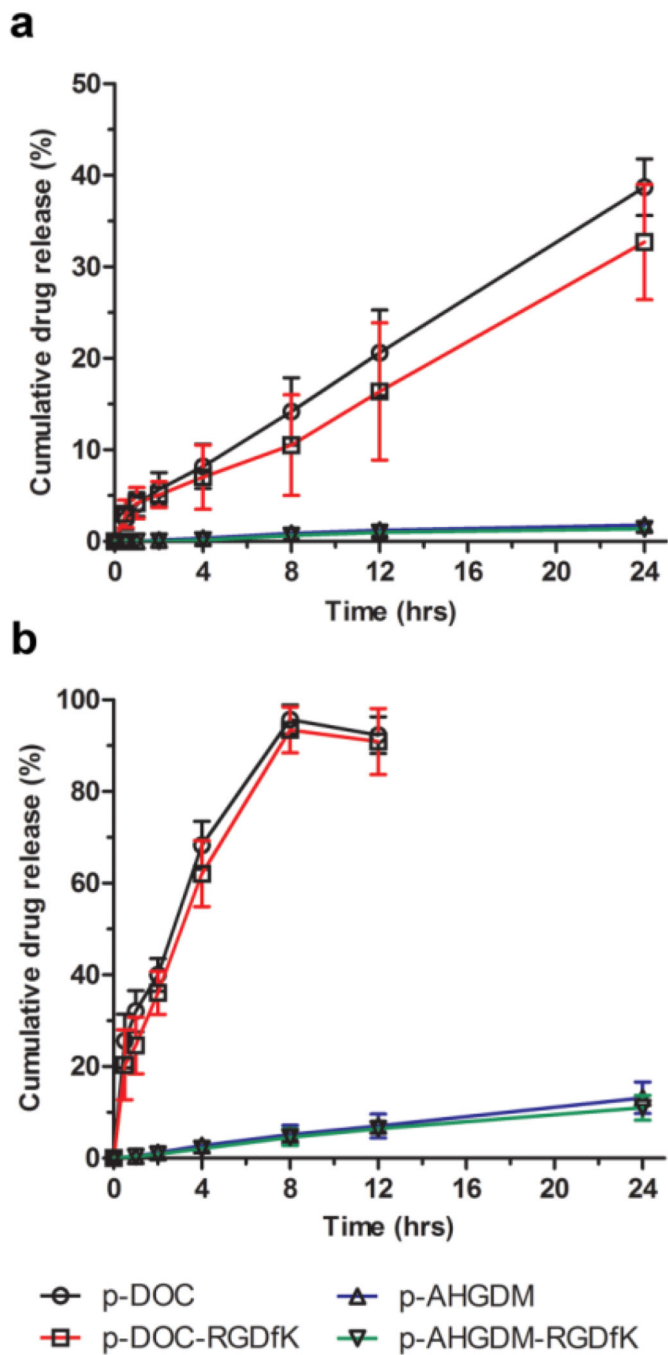


Figure 2. Stability of HPMA copolymer-drug conjugates in PBS and serum

Release of free AHGDM and DOC from HPMA copolymer-drug conjugates as a function of time was assessed in: a) PBS pH 7.4 and b) mouse serum:PBS [1:1]. Release rate was significantly higher for HPMA copolymer-DOC conjugates. Data expressed as mean \pm SD of three independent experiments, with 3 samples per experiment.

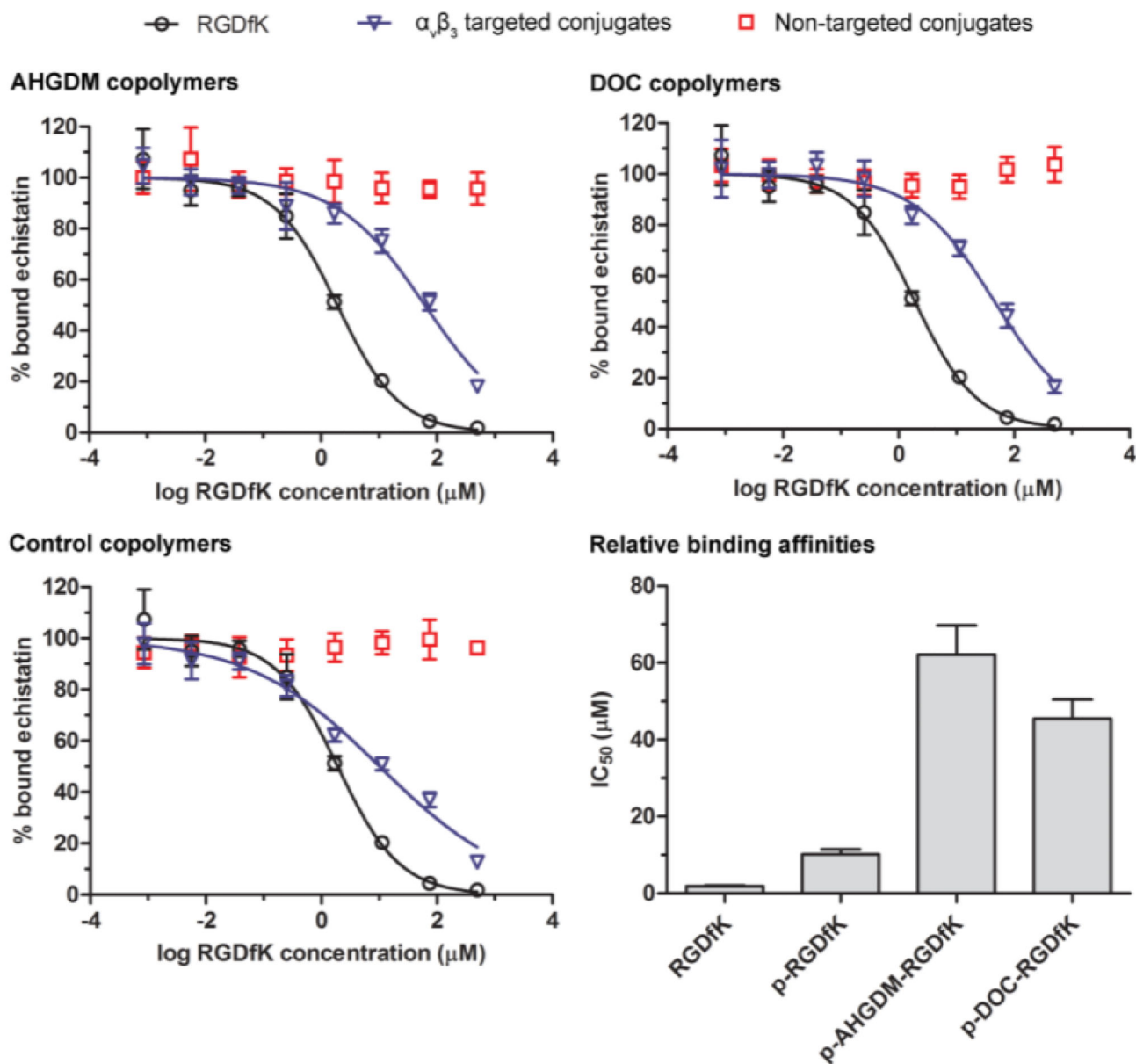


Figure 3. Competitive binding assay of HPMA copolymer conjugates to cell surface $\alpha_v\beta_3$ integrins of A2780 human ovarian cancer cells

All $\alpha_v\beta_3$ targeted conjugates demonstrated the ability to bind $\alpha_v\beta_3$ integrins and all non-targeted conjugates showed no evidence of competitive binding. The relative binding affinity of RGDfK was decreased following conjugation to HPMA copolymers, with drug containing (AHGDM and DOC) copolymers showing a greater reduction in binding affinity as compared to control HPMA copolymers (no drug). Data expressed as mean \pm SD of three independent experiments, with 3 samples per experiment.

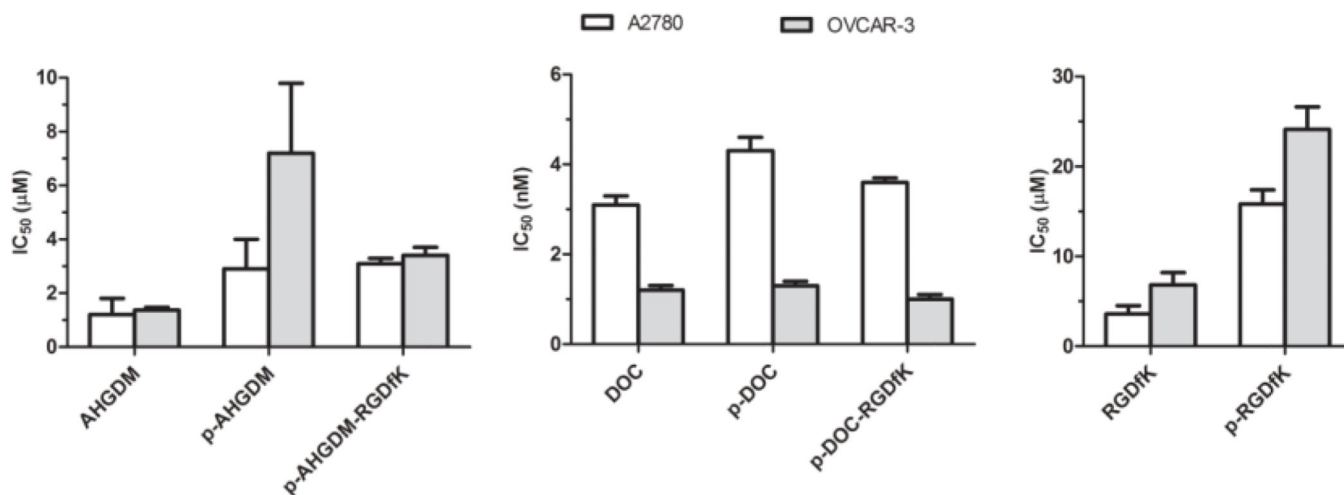


Figure 4. *In vitro* growth inhibition IC₅₀ values of HPMA copolymer conjugates

The ability of HPMA copolymer conjugates to inhibit the growth of A2780 and OVCAR-3 human ovarian cancer cells was evaluated *in vitro*. DOC conjugates exhibited high potency with IC₅₀ values ranging from 1–4 nM, whereas AHGDM conjugates exhibited moderate potency with IC₅₀ values ranging from 3–7 μM. Free RGDfK peptide and control HPMA copolymer-RGDfK demonstrated some potency with IC₅₀ values of 4–7 μM and 16–24 μM respectively. Data expressed as mean ± SD of three independent experiments, with 3 samples per experiment.

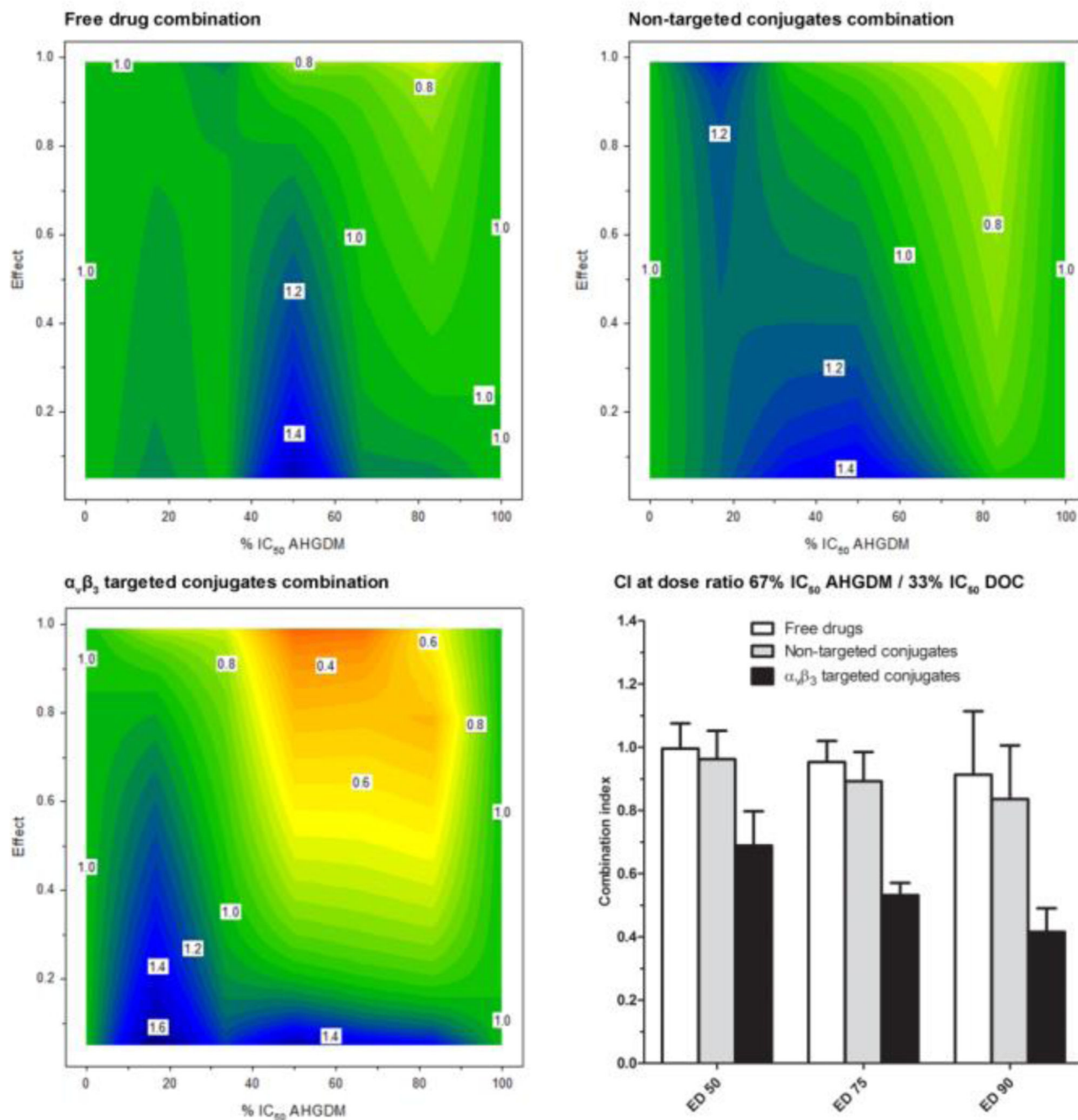


Figure 5. *In vitro* combination index analysis

The combination index (z-axis) was evaluated as a function of drug ratio (x-axis) and effect (y-axis). Three combination treatments were evaluated: 1) Free drug combination (AHGDM + DOC), 2) Non-targeted conjugates combination (p-AHGDM + p-DOC), and 3) $\alpha_v\beta_3$ targeted conjugates combination (p-AHGDM-RGDfK + p-DOC-RGDfK). Various (5) drug ratios were evaluated and effect was defined as $(1 - [\% \text{ relative viability} / 100])$. Combination treatment with $\alpha_v\beta_3$ targeted conjugates demonstrated marked synergism at drug ratios ranging from 50% IC₅₀ AHGDM + 50% IC₅₀ DOC to 83% IC₅₀ AHGDM + 16% IC₅₀

DOC at effect levels above 0.5. A combination treatment of $\alpha_v\beta_3$ targeted conjugates at the optimum drug ratio of 67% IC₅₀ AHGDM + 33% IC₅₀ DOC demonstrated significantly higher synergism as compared to combinations of either non-targeted conjugates or free drugs. Data expressed as mean \pm SD of three independent experiments, with 3 samples per experiment.

Table 1

Characteristics of HPMA copolymer conjugates

Polymer	Description	----- Feed composition - (mol%) -----							Apparent M_w^b (kDa)	M_w M_n	Drug content ^c wt % (% conversion)	RGDFK content ^d wt % (% conversion)
		HPMA	MA- GG- ONp	MA-GG- RGDFK	MA- GFLG- X ^a	MA- Tyr- CONH ₂	MA- Tyr- CONH ₂	MA- Tyr- CONH ₂				
p-AHGDM	Non-targeted AHGDM conjugate	83	10	-	5	2	2	23	1.7	13.9 (85%)	-	
p-AHGDM-RGDFK	$\alpha_v\beta_3$ targeted AHGDM conjugate	83	10	-	5	2	27	1.7	10.6 (84%)	19.3 (82%)		
p-DOC	Non-targeted DOC conjugate	95.5	-	-	2.5	2	20	1.8	7.2 (62%)	-		
p-DOC-RGDFK	$\alpha_v\beta_3$ targeted DOC conjugate	85.5	-	10	2.5	2	23	1.9	6.2 (73%)	17.1 (67%)		
HPMA	Control copolymer	88	10	-	-	2	18	1.6	-	-		
p-RGDFK	Control $\alpha_v\beta_3$ targeted copolymer	88	10	-	-	2	21	1.6	-	21.2 (74%)		

^aWhere X is either AHGDM or DOC;^bEstimated by size exclusion chromatography;^cDetermined by UV spectroscopy for AHGDM and enzymatic release / HPLC for DOC;^dDetermined by amino acid analysis (HPLC).